High Resolution Immunoelectron Microscopic Localization of Functional Domains of Laminin, Nidogen, and Heparan Sulfate Proteoglycan in Epithelial Basement Membrane of Mouse Cornea Reveals Different Topological Orientations

Johannes C. Schittny,* Rupert Timpl,‡ and Jürgen Engel*

* Department of Biophysical Chemistry, Biocenter of the University of Basel, CH-4056 Basel, Switzerland; ‡ Max-Planck-Institut für Biochemie, D-8033 Martinsried, Federal Republic of Germany

Abstract. Thin and ultrathin cryosections of mouse cornea were labeled with affinity-purified antibodies directed against either laminin, its central segments (domain 1), the end of its long arm (domain 3), the end of one of its short arms (domain 4), nidogen, or low density heparan sulfate proteoglycan. All basement membrane proteins are detected by indirect immunofluorescence exclusively in the epithelial basement membrane, in Descemet's membrane, and in small amorphous plaques located in the stroma. Immunoelectron microscopy using the protein A–gold technique demonstrated laminin domain 1 and nidogen in a narrow segment of the lamina densa at the junction to the lamina lucida within the epithelial basement membrane. Domain 3 shows three preferred locations at both the cellular and stromal boundaries of the epithelial basement membrane and in its center. Do-main 4 is located predominantly in the lamina lucida and the adjacent half of the lamina densa. The low density heparan sulfate proteoglycan is found all across the basement membrane showing a similar uniform distribution as with antibodies against the whole laminin molecule. In Descemet's membrane an even distribution was found with all these antibodies. It is concluded that within the epithelial basement membrane the center of the laminin molecule is located near the lamina densa/lamina lucida junction and that its long arm favors three major orientations. One is close to the cell surface indicating binding to a cell receptor, while the other two are directed to internal matrix structures. The apparent codistribution of laminin domain 1 and nidogen agrees with biochemical evidence that nidogen binds to this domain.

B ASEMENT membranes are specialized pericellular matrix structures which underlay endothelial and epithelial cells and surround fat cells, muscle fibers, and peripheral nerves (for a review see reference 64). Basement membranes are responsible for the maintenance and compartmentalization of tissue architecture and their status determines repair after injury. They also provide anchorage for adjacent cells and maintain their polarized and differentiated state. Other functions include the control of cell migration and invasion. Some specialized basement membranes (17) serve as a selective barrier in the filtration of macromolecules.

Basement membranes are composed of glycoproteins, proteoglycans, and collagen. The best characterized components are laminin, nidogen/entactin, the low and high density forms of heparan sulfate proteoglycans, BM-40/SPARC/osteonectin, and collagen IV (for reviews see references 15, 33, 44, 64). Some biologically important functions of basement membranes have been attributed to individual components. Collagen IV forms network structures both in vitro (67, 70)

and in vivo (69). These are believed to provide the scaffold onto which the other components assemble. Laminin is a large multidomain protein of crosslike shape with three short arms and one long arm composed of rodlike and globular structural elements (16). This elongated structure may allow the connection of various matrix components including a tight binding to nidogen (12, 45). Laminin is in addition a well-characterized cell-binding protein (33, 64). Cell adhesion was correlated with inner segments of the short arms (domain 1) and the peripheral portion of the long arm (domain 8) (7, 23, 65). Other important functions of laminin include promotion of neurite outgrowth (13) due to a site localized in the long arm (domain 8), growth promotion (14, 28) and nidogen binding (45) localized in domain 1, and heparan sulfate binding localized in a globular structure at the tip of the long arm (domain 3) which is a substructure of domain 8 (43, 45).

Cross-sectioned basement membranes are visualized at the EM level as continuous thin sheets with a rather amorphous appearance. The epithelial basement membrane of

mouse cornea for example is ~100 nm thick and consists, based on electron density, of a 40-nm-wide lamina lucida at the cellular side that can be distinguished from a somewhat thicker lamina densa facing the stroma. This morphological pattern suggests that basement membranes are deposited by epithelial cells in a polarized fashion typical for many other basement membranes at most other locations. Glomerular and some other basement membranes are, however, exceptional and appear bipolar with two laminae lucida facing epithelial and endothelial cells at opposite sides (17). Immunofluorescence and immunoelectron microscopy have been used to demonstrate the presence of individual proteins referred to above in various basement membranes (for reviews see references 35, 64). So far, only limited information is available on the topological orientations of the components within the basement membrane matrix. This is not too surprising since previous studies were performed with antibodies raised against very large multidomain proteins rather than with antibodies specific for individual domains. Most studies aimed at the immunolocalization of laminin therefore found the protein essentially evenly distributed in the laminae lucida and densa (1-6, 18, 20, 21, 30, 32, 34, 36, 39, 41, 57, 60, 61, 68); while some controversial results indicated a restriction to either the lamina lucida (9, 19) or lamina densa (8, 29, 54).

Because of the assignment of potential biological activities to different domains of laminin by in vitro studies, it is desirable to know whether these domains are in fact found in situ in those positions anticipated from their functions. This specifically refers to laminin domain 1, which binds nidogen and cells, and domains 8 or 3 which bind cells and/or heparan sulfate. We have now used affinity-purified antibodies specific for various laminin domains (7, 13, 43) to determine the topological orientation of this protein in comparison to those of nidogen and heparan sulfate proteoglycan by high resolution immunoelectron microscopy. This was approached by using mouse cornea as model because it possesses a typical well-defined epithelial basement membrane and atypical basement membrane structures underneath the endothelial cell layer (Descemet's membrane) and within the corneal stroma.

Materials and Methods

Preparation of Antisera and Characterization of Affinity-purified Antibodies

All antigens used were prepared from the mouse Engelbreth-Holm swarm tumor (66). Immunization of rabbits and affinity purification of antibodies followed standard protocols (63). Antibodies specific for laminin domain 1 were prepared from antilaminin antisera by immunoadsorption on laminin fragment P1 (7). Antibodies specific for laminin domains 3 and 4 were obtained from antisera against fragments E3 and E4, respectively (13, 43), by passage over adsorbent columns containing the laminin fragment used for immunization. In addition, antibodies reacting with various domains were obtained from an antilaminin serum on a laminin adsorbent. Antisera against nidogen fragment Nd-80 were affinity purified on nidogen fragment Nd-40 which corresponds to the rodlike domain of nidogen (45, 46, 65). Antisera against the low density form of heparan sulfate proteoglycan (11, 49) were purified on an immunoadsorbent containing the intact proteoglycan (49). They react with various domains of the protein core as shown by immunoblotting of tryptic digests of the proteoglycan (data not shown). All purified antibodies were examined by radioimmunoassays (63) and showed strong binding to the desired antigens but not to the other components compared in this study (Table I).

Immunofluorescence Staining

Adult Balb/c mice were killed by cervical dislocation. The eyes were immediately removed, rinsed in PBS, pH 7.4, incubated in Tissue Tek (Miles Laboratories Inc., Naperville, IL) for 5 min, and frozen in liquid nitrogen. Sections of 8 μm were cut with a cryostat-microtome (SLEE, Mainz, FRG) at 20°C, transferred to fat-free microslides, air dried at room temperature, and stored in a dry chamber at −20°C until use.

The sections were rehydrated and stained with 1 μg/ml Hoechst dye (Hoechst, Frankfurt, FRG) in PBS for 10 min, then washed with three changes of PBS containing 20 mg/ml milkpowder (M/PBS) for a total of 1 h. Incubation with affinity-purified antibodies diluted 1:10–1:50 in M/PBS for 1 h was followed by three changes of M/PBS (10 min) and treatment with fluorescein-labeled second antibody (FITC-labeled goat anti-rabbit IgG; Sigma Chemical Co., St. Louis, MO); 1 mg/ml diluted 1:30–1:50 in M/PBS for 1 h. After three more changes of PBS (15 min), sections were embedded in 90% glycerol (E. Merck, Darmstadt, FRG) with 2% propylgallate (Fluka AG, Buchs, Switzerland) including sealing of the cover slip with nail varnish.

All steps were carried out in a moist chamber at room temperature. The stained sections were examined and photographed with appropriate filters to show either the Hoechst dye or the fluoresceine staining.

Tissue Preparation for Immunoelectron Microscopy

Corneas were removed as above and were cut into triangular pieces smaller than 1 mm in PBS containing 0.01 M sodium periodate, 0.05 M lysine, and 2% freshly prepared formaldehyde (37). For ultrathin cryosections, the fixation was stopped after 1 h by immersion of the tissue in PBS containing 1% lysine for 15 min. Plain PBS was used for freeze substitution.

Labeling of Ultrathin Cryosections

Fixed samples were frozen in a mixture of 70% liquid propane and 30% isopentane cooled by liquid nitrogen to −196°C followed by sectioning and labeling (25). Specifically, after cutting with a microtome (LKB Instruments, Inc., Stockholm, Sweden) and picking up individual sections on EM grids, they were stored on a gel of 2% gelatin containing PBS at 4°C for 1–72 h. Before labeling, grids were washed three times for 3 min on drops of PBS containing 1% lysine, and once for 5 min on drops of PBS with 10% FCS (Gibco AG, Basel, Switzerland). The grids were then incubated with the specific antibody for 1 h. The antibody stock solution (0.4–1.6 mg/ml) was diluted 1:1–1:20 with PBS. The final solution contained 0.1% Tween 20, 0.1% Triton X-100, and 2% milk powder. Grids were then washed six times for 15 min on drops of PBS, incubated for 30 min with a solution of protein A-gold (reduced with ascorbate according to reference 52) in PBS containing 0.1% Tween 20, 0.1% Triton X-100, 1% gelatin and 1% bovine albumin. A final washing with PBS and distilled water and the embedding in methylcellulose was done as described by Griffiths et al. (25). All operations were performed at room temperature.

Freeze Substitution and Embedding in Lowicryl

The tissue was frozen with a high pressure freezing apparatus (model HPM 010; Balzers AG, Liechtenstein) according to Moor et al. (40). Samples were stored in liquid nitrogen, substituted in pure acetone at −85°C, embedded in a graded series of Lowicryl K₁₁M at −60°C, and polymerized with UV light at either −60°C or room temperature for 2 d each (58).

Labeling of the Plastic Sections

Labeling followed a previously described protocol (52). The unspecific binding of the antibody was blocked with M/PBS for 5 min. Stock solution of the affinity-purified antibodies were diluted 1:1–1:20 in PBS containing 0.1% Tween 20, 0.1% Triton X-100, and 2% milk powder. The grids were incubated with this solution at room temperature for 1–2 h. Treatment with protein A-gold was done as described for the cryosections. The counterstaining was done with saturated uranyl formate at a series of five to seven drops, each applied for 1 min, followed by a brief washing with distilled water.

---

1. *Abbreviations used in this paper:* LDPG, low density heparan sulfate proteoglycan; M/PBS, phosphate buffered saline containing milk powder.

Table I. Specificity of Affinity-purified Antibodies Against Laminin and Laminin Fragments

Immunogen	Affinity column	Antibody concentration	Antigen-binding capacity for ¹²⁵I-labeled			
			laminin	fragment 1	fragment 3	fragment 4
		mg/ml	*μg/ml*	*μg/ml*	*μg/ml*	*μg/ml*
Laminin	Laminin	0.6	21	17	7	0.7
Laminin	Fragment 1	1.4	53	40	<0.1	<0.1
Fragment 3	Fragment 3	1.3	31	<0.02	35	<0.02
Fragment 4	Fragment 4	1.6	40	0.2	<0.1	53

Statistical Evaluations

Measurements were performed on enlargements magnified 36,000 times. For determining the density of label, gold grains were counted in an area of 25–50 μm² (stroma), 15–40 μm² (Descemet's membrane), and 2.2–5.5 μm² (basement membranes) for each individual section. Areas were measured by an Apple IIe computer equipped with a graphics tablet (Apple Computer Inc., Cupertino, CA). Because epithelial basement membranes were too thin for a direct determination of their areas, it was determined by multiplying the length evaluated by the mean diameter (100 nm).

For evaluating histograms of label distribution across the width of the epithelial basement membrane, its diameter was defined as the distance between the plasma membrane at the cellular side and the junction to the corneal stroma. At the position of each label, the diameter was divided into eight equal length intervals of which five correspond to the lamina densa (64 ± 2% of the diameter) and three to the lamina lucida. The position of each individual grain was assigned to one of the eight intervals. This method implies a normalization of the absolute diameter (100 ± 17 nm) accounting for variations most probably caused by oblique sectioning, due to undulations of the inner ocular surface of the corneal epithelium. For each experiment the positions of 155–440 gold grains were counted.

Results

Domain Specificity of Purified Antibodies

Polyclonal antibodies specific for domains 1, 3, or 4 were used for the labeling of distinct portions of the laminin molecule (Fig. 1). The antibodies were prepared from rabbit antisera against laminin or the laminin fragments 1, 3, and 4 corresponding to the domains whose localizations are indicated by the same numbers in Fig. 1. The antibodies showed strong binding to the corresponding fragment in radioimmunoassays and negligible reactions with the unrelated fragments (Table I). They also failed to react with nidogen and the proteoglycan. For further characterization of earlier preparations of the same antibodies see Ott et al. (43).

Antinidogen antibodies were also used for labeling since nidogen is closely associated to the central domain 1 of laminin (Fig. 1) in stable and stoichiometric complexes (45). The antinidogen antibody was affinity purified on a nidogen fragment corresponding to its rodlike domain (Fig. 1) and showed complete cross-reaction and strong binding to intact nidogen (46). Since nidogen binds to laminin by one of its globular domains (Fig. 1), the antibodies have access to the epitopes even after complex formation with laminin (45). Purified antibodies against the low density form of basement membrane heparan sulfate proteoglycan (LDPG) were added to the repertoire of markers because of the importance of this proteoglycan for the function and molecular organization of basement membranes (48, 49). The antibody reacts exclusively with the protein core of the proteoglycan (11) which consists of six globular domains arranged in an 80-nm-long

segment of 500 kD (49). Preliminary evidence indicates that the antibodies bind to several if not all of the domains within the protein core. These antibodies failed to react with the other basement membrane proteins examined here (11, 49) and with collagen type IV.

Localization of Basement Membrane Components in the Mouse Cornea by Indirect Immunofluorescence

The histological distribution of laminin (Fig. 2, *a* and *b*), nidogen (Fig. 2, *c* and *d*), and LDPG (Fig. 2, *e* and *f*) in mouse cornea was studied by indirect immunofluorescence on unfixed cryosections and revealed almost identical staining patterns. Staining is restricted to epithelial basement membrane, small plaques located in the corneal stroma, basement membranes surrounding nerve fibers, and Descemet's membrane. The latter often appears as a segment encased by two stained lines (Fig. 2, *a* and *b*) which may, however, be an artifact since it is not supported by immunoelectron microscopy (see below). This artificial staining pattern could be caused by ice crystal growth during freezing. When antibodies against laminin, nidogen, and LDPG were incubated with their respective soluble antigens before application, fluorescence staining of discrete structures was abolished, and only a weak unspecific background was seen (not shown). This unspecific staining was comparable to the weak staining observed with a nonimmune rabbit IgG. Immunofluorescence was also used as a convenient test for selecting antibodies to be used in immunoelectron microscopy. Only those preparations which produced a bright and specific fluorescence at concentrations below 50–100 μg/ml were found to produce sufficient label density in immunoelectron microscopy.

General Features of Immunoelectron Microscopy on Ultrathin Cryosections

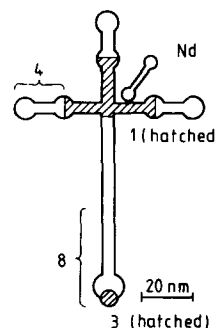Immunoelectron microscopy was applied primarily for the

Figure 1. Localization of fragments 1, 3, 4, and 8 within the crosslike structure of laminin and approximate position of the dumbbell-shaped nidogen molecule in the laminin/nidogen complex (based on references 16, 43, 45).
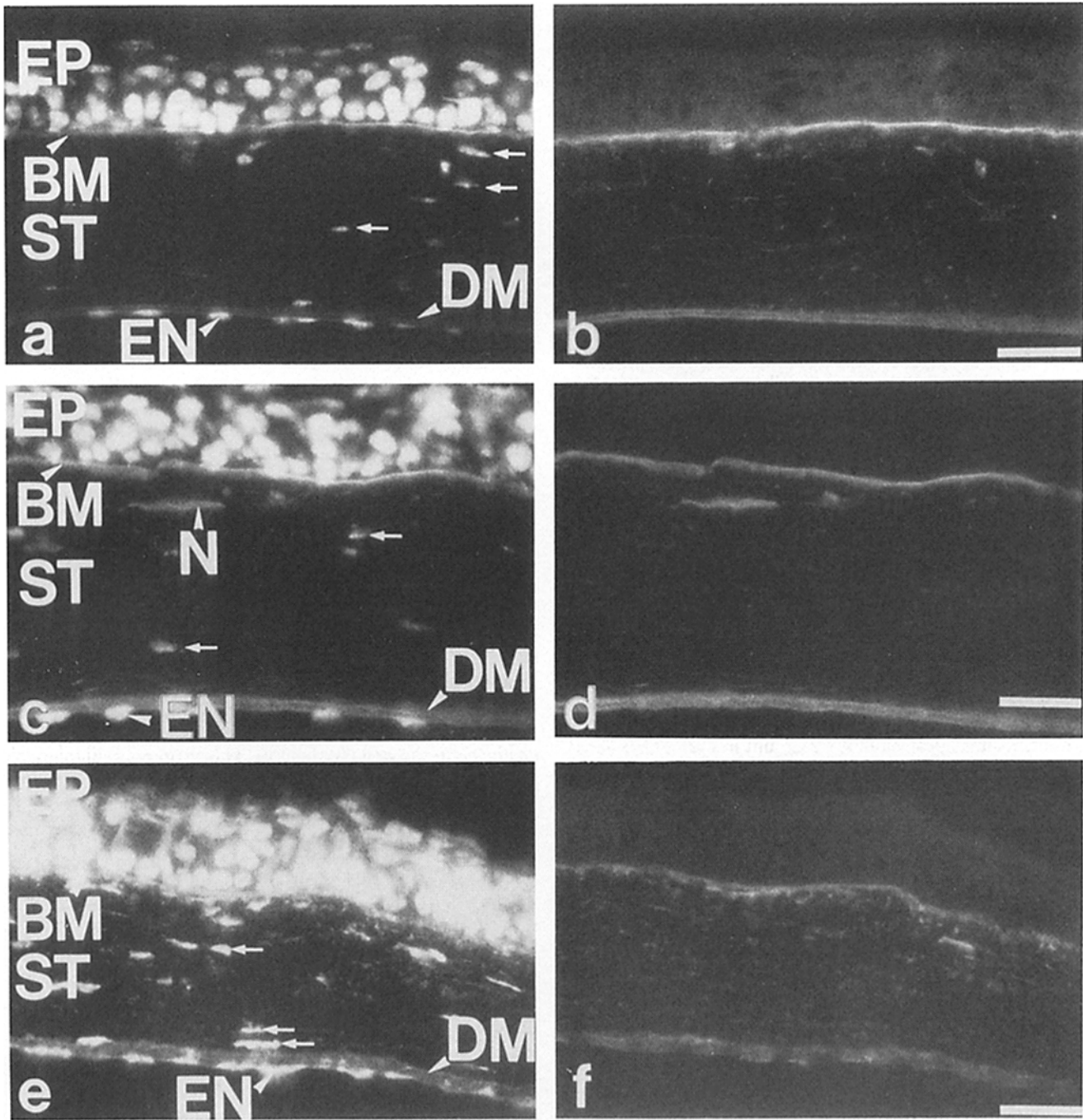
Figure 2. Immunofluorescence localization of laminin (*a* and *b*), nidogen (*c* and *d*), and heparan sulfate proteoglycan (*e* and *f*) in the mouse cornea. Unfixed cryostat sections were labeled with antilaminin, antinidogen, and anti-LDPG antibodies, respectively, and stained with FITC–anti–rabbit IgG. (*a*, *c* and *e*) Epithelial (*EP*), endothelial (*EN*) cells, and fibroblasts (*arrows*) are, in addition, visualized by chromosome staining with Hoechst dye (originally distinguished from FITC staining by its blue fluorescence). For all three proteins staining is seen in the epithelial basement membrane (*BM*), in small plaques located in the stroma (*ST*), around nerves (*N*), and in Descemet's membrane (*DM*). Bars, 25 μm.

localization and identification of individual domains of laminin and of nidogen and LDPG in cross sections of the epithelial basement membrane. Since plaques in the stroma and Descemet's membrane apparently also contain laminin, nidogen, and LDPG these structures were examined for comparison.

Protocols for specimen preparation had to be optimized

for immunoreactivity and structure preservation. Cryosectioning offered the best compromise between these goals, allowing label densities which were sufficiently high for an evaluation of the distribution of all antigens (Table II). Protein A–gold was used for labeling because of the advantage it afforded: bound antibody molecules are labeled by single gold grains (52) and not by clusters as in the case of IgG–gold

complexes. Background labeling comprised only 1–16% of the specific labeling (Table II). Embedding in Lowicryl K₁₁M after freeze substitution resulted in a better structure preservation but somewhat less label density as compared to cryosections and was also used in some cases.

Basement Membrane of the Corneal Epithelium

Electron micrographs of ultrathin cryosections labeled with the different antibodies are shown in Fig. 3. The basement membrane is located between the epithelium (*EP*) and the corneal stroma (*ST*). It is divided into the lamina lucida (*LL*) at its cellular side and the lamina densa (*LD*) at its extracellular side. Differences in labeling patterns are visible already by visual inspection. Antilaminin (Fig. 3 *a*) and anti–LDPG antibodies (Fig. 3 *f*) which react with a large variety of domains produce rather uniform distributions with the highest number of labels per μm^2 (Table II). The labeling with antibodies against a particular nidogen domain and with antibodies against several domains of laminin resulted in weaker but clearly significant signals. Domain 1 of laminin (Fig. 3 *b*) as well as nidogen (Fig. 3 *e*) appear to be located in the central region of the basement membrane, whereas laminin domains 3 and 4 appear in the lamina lucida and in most parts of the lamina densa.

For a more objective and quantitative evaluation of the results, a statistical analysis of the micrographs was performed (Fig. 4). The labeling by antilaminin antibodies appears all over the cross section of the basement membrane with a slight accumulation in its central part (Fig. 4 *a*). In striking contrast, the label frequency for domain 1 of laminin exhibits a sharp peak with a maximum in the lamina densa at the junction to the lamina lucida. Labeling for the small (Fig. 4 *b*) domain 3 exhibits a more uniform distribution with three maxima at both borders of the basement membrane and in its center (Fig. 4 *c*). Domain 4 appears to be predominantly present in the lamina lucida and in the adjacent half of the lamina densa (Fig. 4 *d*).

The frequency distribution of the labels for nidogen (Fig. 4 *e*) is very similar to the one for laminin domain 1 (Fig. 4 *b*). Both are found to be located at the borderline between the lamina densa and the lamina lucida with a maximum slightly inside the lamina de. ι. Labels for LDPG are detectable in regions across the basement membrane except for a distinct decrease at its most cellular side (Fig. 4 *f*). This contrasts to a higher label density at the borderline to the corneal stroma.

The labeling pattern in the direction parallel to the plane of the basement membrane was searched for repeats. In the case of antibodies to laminin domain 1 and nidogen, where the labels are deposited approximately in a row, the distances between the single gold grains were measured over a total length of ∼25 μm. For none of the antigens could periodicity of the labels be detected either by statistical analysis or by visual inspection.

Basement Membrane-like Plaques in the Corneal Stroma

The basement membrane components laminin (Fig. 5), nidogen (Fig. 5 *e*), and heparan sulfate proteoglycan (not shown) are localized in distinct areas of the corneal stroma. They were detected in amorphous elongated structures, which ap-

Table II. Density and Specificity of Antigen Labeling in Ultrathin Cryosections of Mouse Cornea

Antibody against	Epithelium	Basement membrane	Stroma	Descemet's
Laminin	0.7	88.0	2.9	42.0
inhibited	<5.0	<10.0	1.1	1.9
Domain 1	2.5	49.0	1.1	13.0
inhibited	9.6	6.5	1.0	1.5
Domain 3	4.0	46.0	5.1	11.0
inhibited	2.9	4.9	2.3	1.5
Domain 4	2.3	53.0	3.7	27.0
inhibited	4.0	8.4	9.5	4.1
Nidogen	2.0	43.0	2.6	18.0
inhibited	1.9	2.7	2.0	3.0
LDPG	1.1	60.0	1.9	34.0
inhibited	0.8	0.1	0.3	0.7
Nonimmune rabbit IgG	0.4	0.9	0.4	0.0

The density of gold labels is given in grains per μm^2. The SD is smaller than ± 3 labels/μm^2. In the inhibition test, the specific antibody was incubated with its soluble antigen before application.

pear morphologically similar to the lamina densa. Some of these elongated elements are apparently in contact with one side of fibroblasts (Fig. 5, *a* and *b*), whereas others are localized between large cross-striated collagen fibers (Fig. 6, *c*–*e*). The latter plaques did not show any apparent contact with typical basement membranes or with cells. Such plaques, as indicated by the immunofluorescence, are homogeneously distributed throughout the whole corneal stroma (Fig. 2, *a*–*c*). They are clearly distinct from basement membranes around peripheral nerves, which are always in contact with nerve and/or Schwann cells, divided into a lamina densa and a lamina lucida zone, and are perhaps related to the collagen IV– and laminin-containing structures observed by Pratt and Madri (50).

Distribution of Antigens in Descemet's Membrane

In contrast to the basement membrane of the corneal epithelium (see above), all studied proteins or their fragments were found to be homogeneously distributed in the Descemet's membrane (Fig. 6). No significant correlation of the labels to any structural element of this membrane could be detected. In particular, there was no indication of a labeling pattern which could comprise the double line observed by immunofluorescence staining of Descemet's membrane (Fig. 2).

Discussion

Immunoelectron microscopic studies with antibodies directed against individual domains of laminin provided new insights on possible arrangements of this large multidomain protein which could not be obtained in previous work with antibodies directed against the whole laminin molecule (20, 21, 30, 34, 35, 38, 39, 54, 60). The present work concentrated on epithelial basement membranes of mouse cornea because of their typical morphological appearance and di-
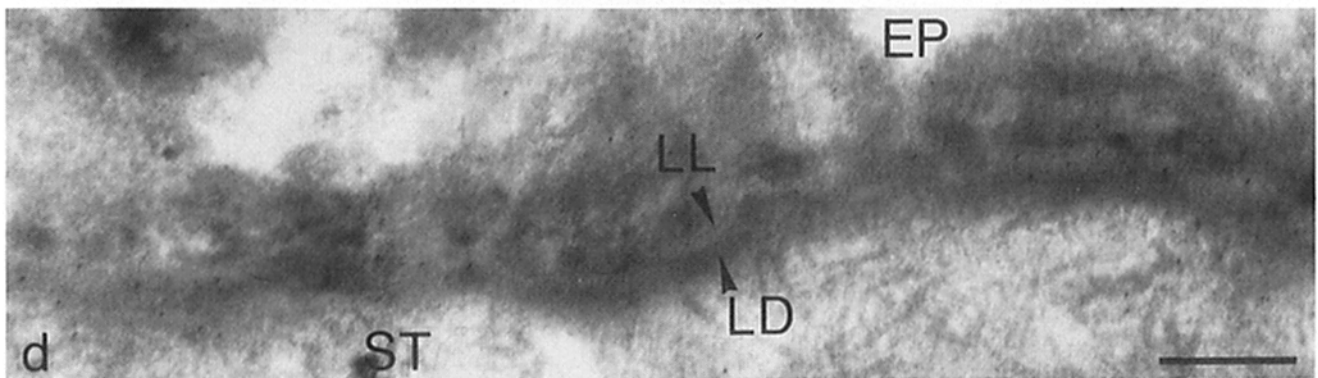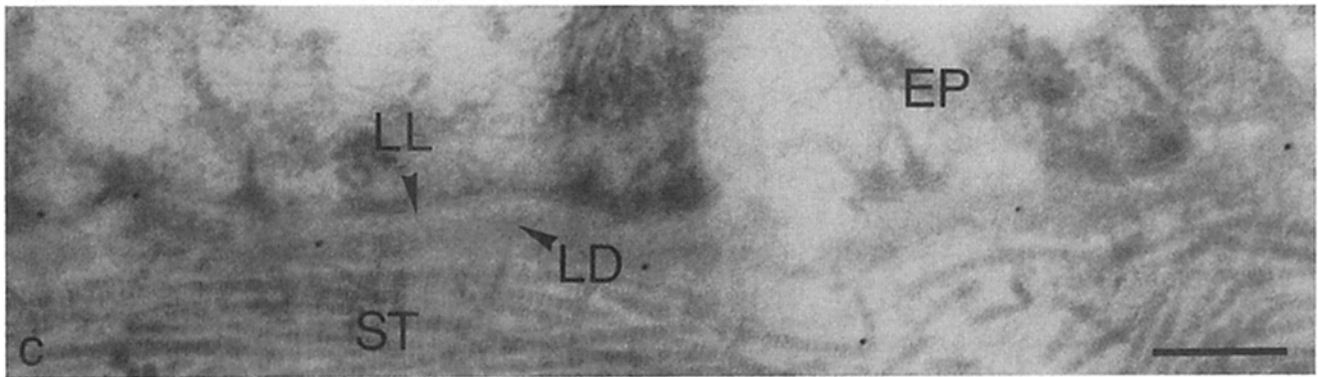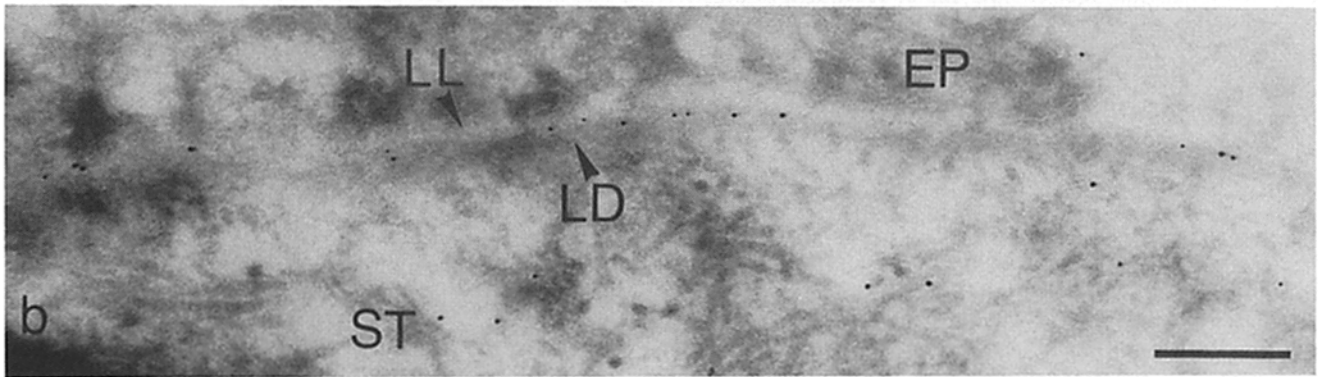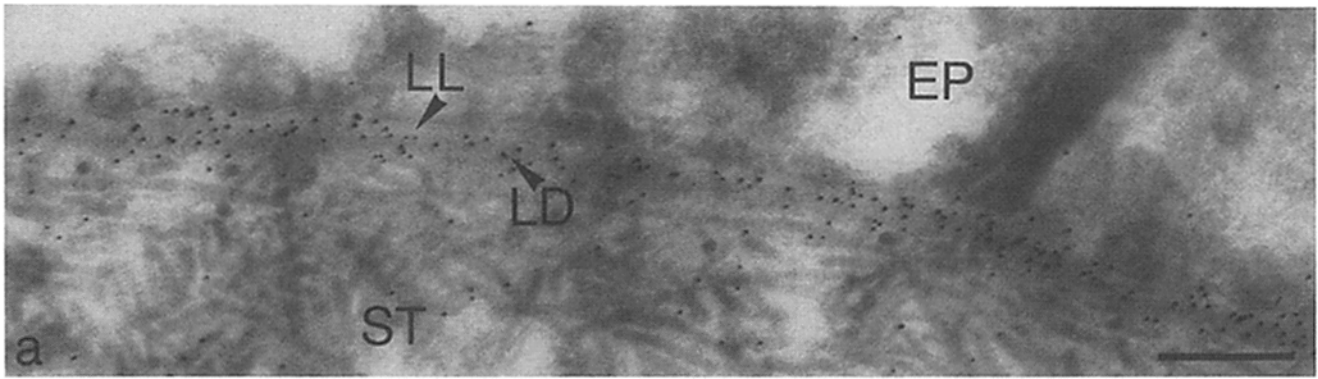
Figure 3. Localization of laminin, nidogen, and proteoglycan in the basement membrane of the corneal epithelium. Ultrathin cryosections of the mouse cornea were labeled with antilaminin antibodies (*a*), antibodies against individual domains 1 (*b*), 3 (*c*), and 4 (*d*), of laminin, and antibodies against nidogen (*e*) and proteoglycan (*f*). Nonimmune rabbit IgG was applied in control experiments (*g*) using the protein A–gold technique. *EP*, epithelium; *LD*, lamina densa; *LL*, lamina lucida; *ST*, stroma. Bars, 0.3 μm.
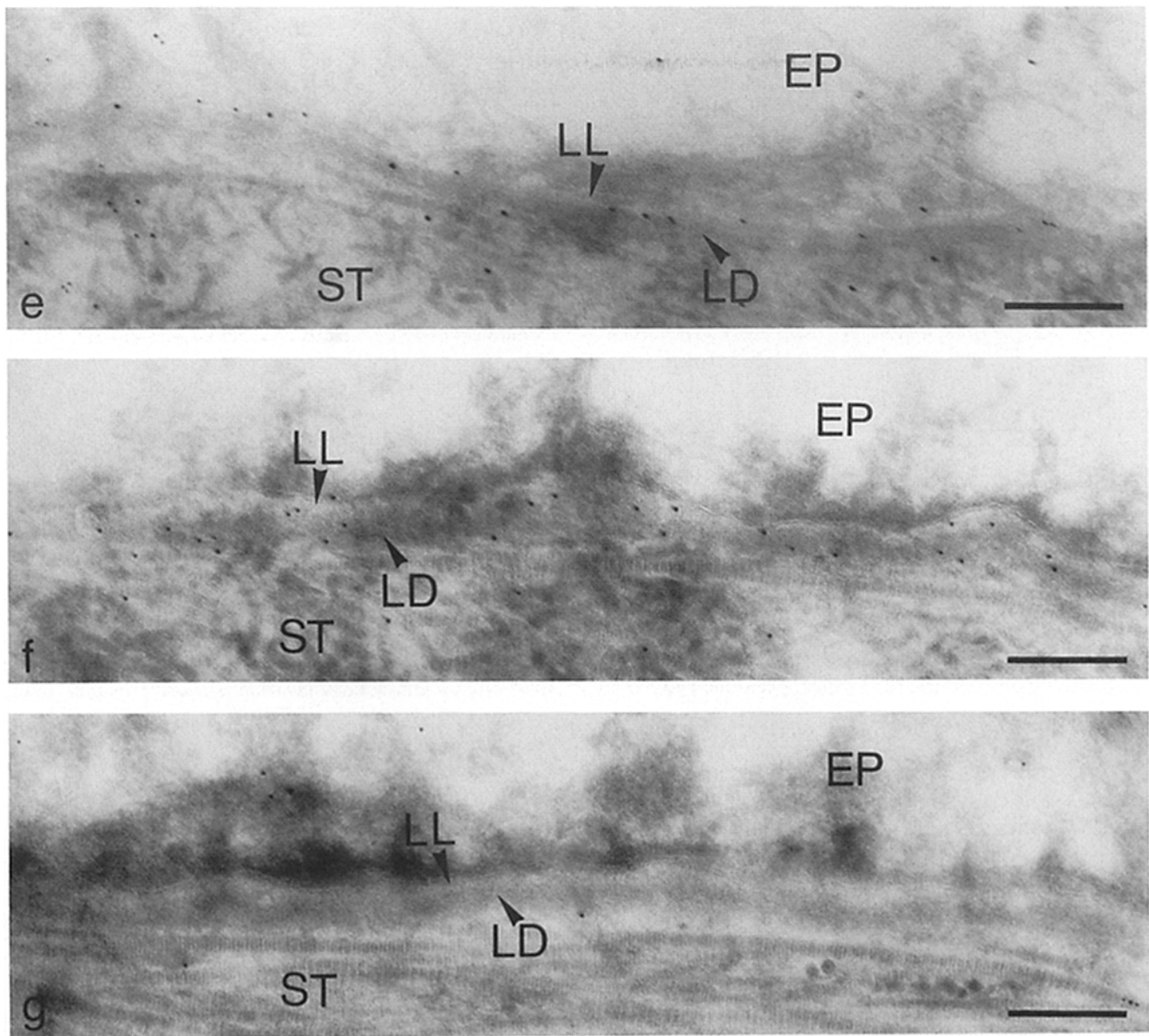
Fig. 3 (e–g)

ameter, whereas several of the earlier studies have used the much thicker Reichert's membrane (59) or the bipolar glomerular basement membrane. (1, 3–5, 8, 9, 20, 29, 32, 36, 41). There may exist large differences between the supramolecular organizations of these matrices although they share major basement membrane constituents including laminin.

In the epithelial basement membrane of mouse cornea, a well-defined lamina lucida facing the cell surface can be distinguished from a lamina densa facing the stroma. The lamina lucida comprises ∿1/3 of the total diameter of 100 ± 17 nm. It has been argued that division in the two zones reflects fixation and staining artifacts (22). They were, however, observed in the present study by rather different methods of specimen preparation and have been generally observed for a large number of typical basement membranes by a variety of techniques. We further show here by high resolution protein A–gold technique that both layers differ also in the exposure of different laminin domains.

The central domain 1 of laminin seems clearly located near the junction between the two laminae in a narrow segment (25–35 nm) containing >80% of the total label. This corresponds well to the dimensions of domain 1 which consists of three 20-nm-long rodlike segments originating from three short arms of laminin (16, 43). Sequence analyses (55, 56) demonstrated that these regions consist of cysteine-rich repeats which exhibit restricted homology with epidermal growth factor. Domain 1 promotes cell attachment in vitro (7, 33, 62), and a specific cellular receptor (M_r 67,000) possibly mediating this interaction was described (31, 33, 51). Recently a mediator function for cell attachment, chemotaxis, and receptor binding was reported for a nonapeptide which was synthesized according to the sequence of the B1 chain segment present in domain 1 (24). All these functions are difficult to reconcile with the distribution of immunolabels for domain 1 in the intact basement membrane, indicating that it is not exposed to cells. This apparent dis-
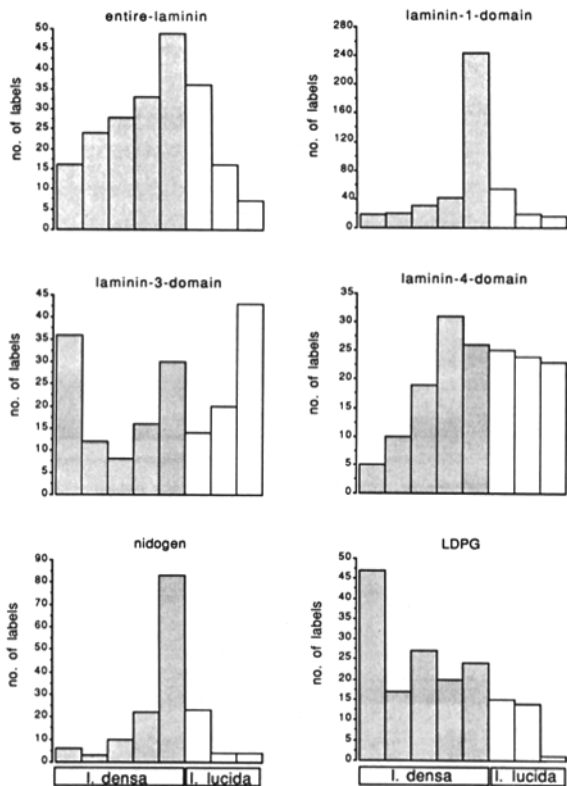
Figure 4. Histograms of antibody distributions against laminin; its domains 1, 3, and 4; and against nidogen and LDPG in cross sections of the cornea epithelial basement membrane. Data were evaluated from electron micrographs like those shown in Fig. 3. Eight intervals of equal length were defined across the diameter of the basement membrane (∼100 nm) of which five correspond to the lamina densa and three to the lamina lucida. The number of gold particles falling into these intervals was determined for a total of 155–440 grains in each experiment.

crepancy can, however, be explained by more recent observations showing that domain 1 is only active in cellular interactions when released by proteolysis but is apparently much less accessible in intact laminin (42). This concept of a cryptic cell-binding site may also be applicable to a growth factor-like activity which was recently attributed to domain 1 (14). Such properties could be expressed during biosynthesis and morphogenesis before completion of the intact basement membrane structure and in the case of partially disassembled basement membranes in tissue repair.

The localization of domain 1 of laminin in the interior of the basement membrane shows a satisfying coincidence with the localization of nidogen. This protein which is most likely identical or very closely related to entactin (47) forms a very stable equimolar complex with laminin (12, 45). Complex formation occurs by the binding of one of the globular domains of nidogen to domain 1 of laminin. The restriction of the immunolabel is also compatible with the length of the dumbbell-shaped nidogen molecule which does not exceed 20 nm (45). In view of its tight association to laminin and other properties, nidogen has to be considered as an integral structural protein of basement membranes. Its central position in the epithelial basement membrane examined here is in accordance with this view.

It has been recently reported (7, 23) that domain 8 in laminin contains a more potent and commonly recognized site for cellular interactions than domain 1. In fact domain 8, as monitored by immunolabeling of domain 3 at the tip of the long arm, showed the highest abundance near this surface of epithelial basement membrane which faces the cells. Domain 8 is therefore a more likely candidate for being involved in the interactions between cells and intact basement membranes than domain 1. This is also in agreement with other data showing that domain 8 but not domain 1 inhibits cell binding of laminin in a competitive manner (Nurcombe, V., M. Aumailley, R. Timpl, and D. Edgar, unpublished data).

Another function which is attributed to domain 8 is the well known neurite outgrowth promotion by laminin (13). Neurite growth promotion is also expressed by intact basement membranes (10, 53) suggesting that the active part of domain 8 is indeed exposed.

Further maxima of domain 3 distribution are observed in the central region and at the stromal side of the lamina densa. We therefore conclude that the long arm of laminin is present in several orientations which are illustrated in a schematic way in Fig. 7. These variable orientations of the long arm could reflect its potential to bind heparan sulfate which has been previously attributed to domain 3 (43). The rather broad distributions observed by immunolabeling of the entire laminin molecule and of domain 4 are consistent with this schema but it is impossible to derive details of the supramolecular organization or exlude other possible arrangements on the basis of the present data. It should be noted that domain 4 is present at high abundance close to the cellular surface but did not extend to the stromal side of the basement membrane. This could be due to the maximal distance of 37 nm between the peripheral end of domain 4 and the center of the laminin cross as represented by domain 1 (16).

Spacings between labels showed no periodicity which could have provided clues for an ordered assembly. The network structure of collagen IV was recently revealed in considerable detail in basement membranes of amniotic epithelium (69). Here again no clear periodicities were visible which was interpreted as indicating that the supramolecular organization of collagen IV exhibits considerable plasticity. This may also be true for laminin which is thought to bind to the collagen IV scaffold.

Periodic patterns were reported for a heparan sulfate proteoglycan in glomerular basement membranes after ruthenium red staining (27) which reacts with collapsed heparan sulfate chains to some extent after immunolabeling (35). This proteoglycan was found to be restricted to the laminae lucida interna and externa. It is not known how the glomerular heparan sulfate proteoglycan is related to the large LDPG which was isolated from Engelbreth-Holm swarm tumor tissue (49). With antibodies to the protein core of LDPG we found a rather homogenous distribution in both laminae with some preference for the lamina densa. No periodicity of the labels was detectable in the direction parallel to the plane of the basement membrane. LDPG has an extended, ∼80-nm-long protein core with six globular domains in a row (49), and three heparan sulfate chains attached to a terminal domain. From the present data it cannot be decided whether the LDPG protein core to which our antibody is directed spans the basement membrane or whether other possible ar-
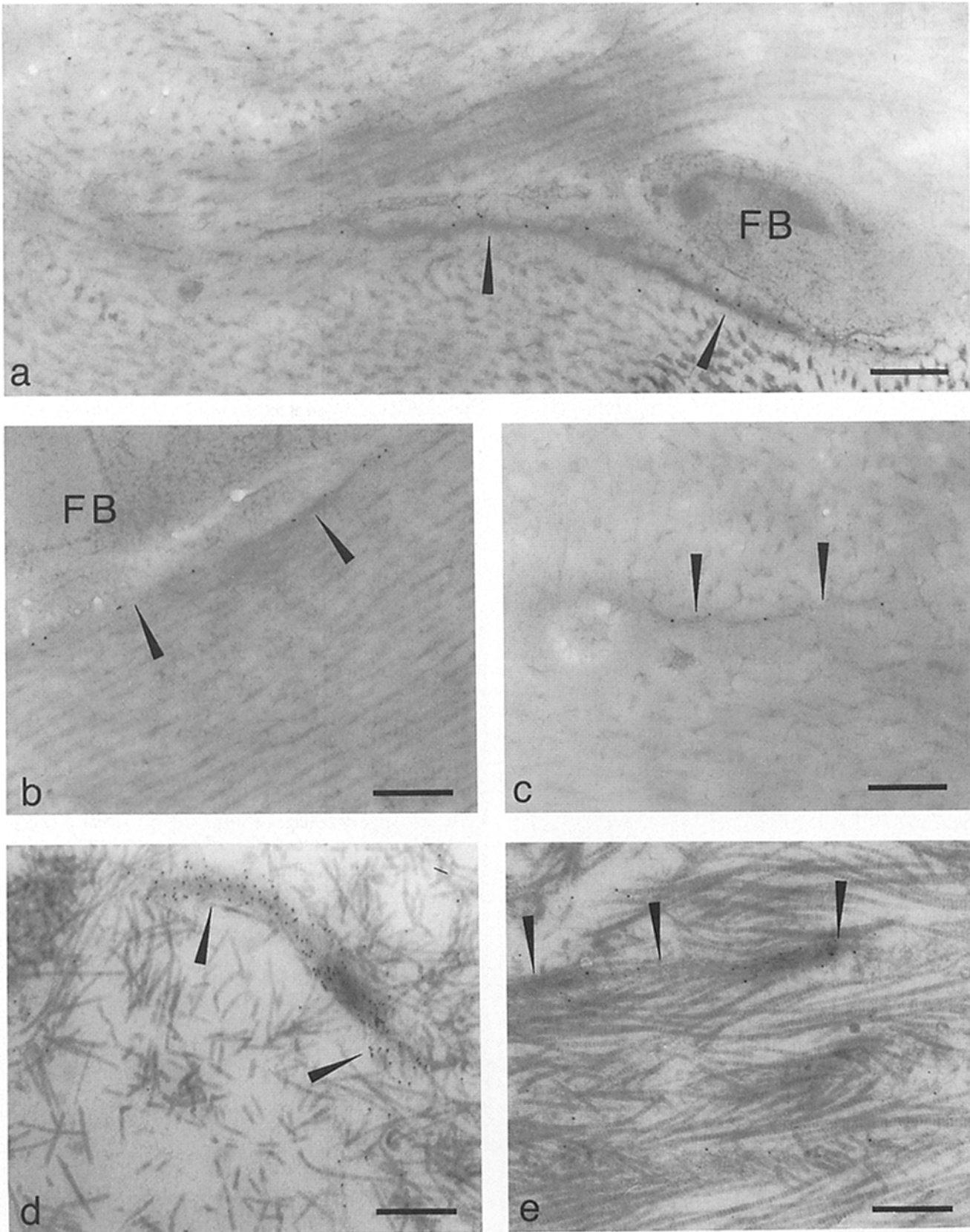
Figure 5. Localization of laminin and nidogen in basement membrane–like plaques located in the corneal stroma. Such plaques (*arrows*) were often in contact with fibroblasts (*a* and *b*; *FB*) or associated with large collagen fibers (*c*, *d*, and *e*). Sections of plastic (K₁₁ M), embedded freeze-substituted material (*a*, *b*, and *c*), or ultrathin cryosections (*d* and *e*) were treated with antilaminin (*a*, *b*, *c*, and *d*) or antinidogen (*e*) antibodies, and the markers were visualized by protein A–gold.
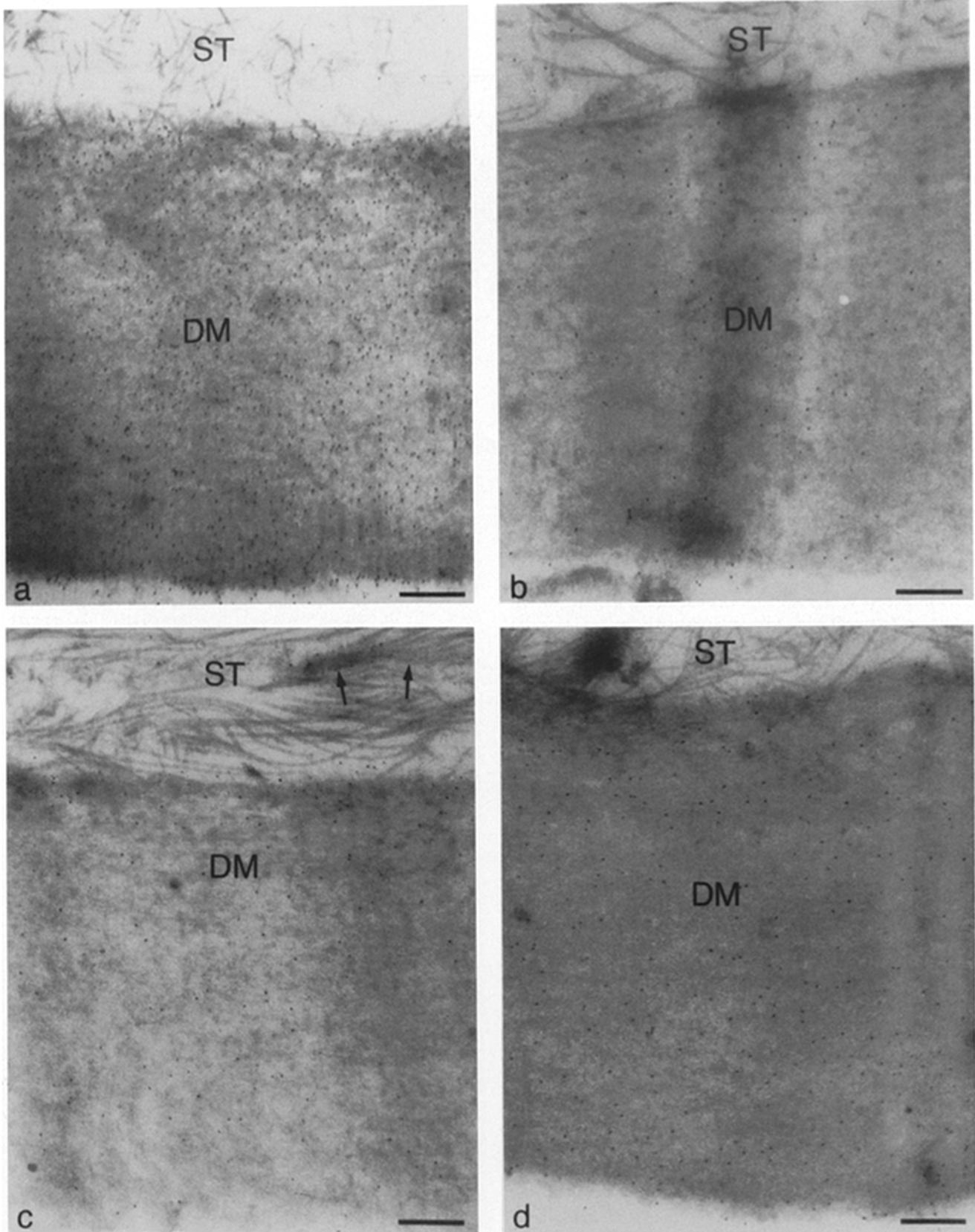
Figure 6. Localization of laminin, nidogen, and proteoglycan in Descemet's membrane. Ultrathin cryosections of the mouse cornea were labeled with antibodies against laminin (*a*), its domain 1 (*b*), nidogen (*c*), and proteoglycan (*d*) using the protein A–gold technique. A rather homogeneous distribution of the labels is seen in all cases. Similar results have been obtained with antibodies against laminin domains 3 and 4 (not shown). *DM*, Descemet's membrane; *ST*, stroma; *arrows*, basement membrane–like plaques (see Fig. 5). Bars, 0.4 μm.
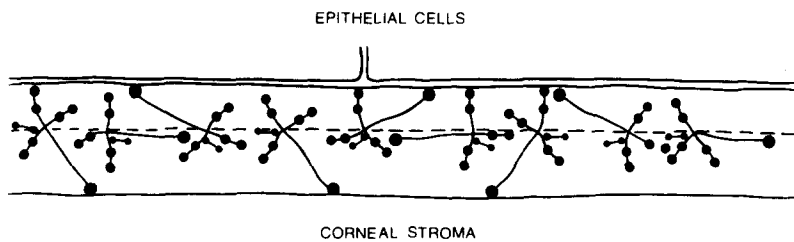
EPITHELIAL CELLS

CORNEAL STROMA

Figure 7. Scheme of possible orientations of the laminin/nidogen complex (see Fig. 1) in cross sections of the epithelial basement membrane which is consistent with the observed distribution of domains 1, 4, and 3 and of nidogen. The highly schematic drawing does not account for a possible arrangement of the laminin arms and of nidogen in three dimensions. Dashed line indicates the border between lamina lucida and lamina densa.

rangements account for the uniform distribution. These questions may be addressed by immunolabeling of distinct domains of the protein core by suitable antibodies not yet available.

The characteristic distribution of laminin domains observed here for cornea epithelial basement membrane may reflect its two layer morphology and average thickness of ~100 nm. Whether other basement membranes with a similar morphology but different anatomical localization will exhibit a comparable domain distribution remains to be studied. Due to the dynamic nature of basement membranes, the distribution may also depend on the stage of development. Additional complexity may be introduced by the possible presence of isoforms of laminin and other basement membrane components. Laminins with distinct differences in shape and chain composition were found to be secreted by some specialized mammalian cells and are also found in invertebrate tissues (reviewed in reference 33) but no information is available on isoforms in epithelial basement of the cornea. The restriction of laminin domain 1 and nidogen to a narrow section within the lamina densa also raises the question on masking effects. Studies with antilaminin and anti–domain 3 antibodies demonstrated availability of epitopes over the whole width of the cross-sectioned basement membrane. If masking accounts for the restricted labeling of domain 1 and nidogen, then it should be a very specific effect both in terms of ultrastructural localization and the structures involved. Studies with antibodies against other laminin domains and/or individual epitopes may help to settle this point and provide a more refined picture of laminin orientations.

With all the antibodies used here, rather uniform labeling patterns were observed on Descemet's membrane. This unique extracellular membrane has a thickness of several micrometers and possesses hexagonal and cross-shaped morphological structures (26) not observed in other basement membranes. Our data suggest a highly variable orientation of laminin in Descemet's membrane. Basement membrane–like plaques in the corneal stroma which lack a lamina lucida also showed irregular antibody-labeling patterns of rather low density. These few examples indicate that different basement membranes may become distinguishable not only by morphological criteria but also by the topography of their common constituents.

References

1. Abrahamson, D. R. 1986. Lamina rara interna, lamina densa, and lamina rara externa of renal glomerular basement membrane. *J. Histochem. Cytochem.* 34:847-853.
2. Abrahamson, D. R., and J. P. Caulfield. 1982. Proteinuria and structural alterations in rat glomerular basement membranes induced by intravenously injected anti-laminin IgG. *J. Exp. Med.* 156:128-145.
3. Abrahamson, D. R., and J. P. Caulfield. 1985. Distribution of laminin within rat and mouse renal, splenic, intestinal, and hepatic basement membranes identified after the intravenous injection of heterologous antilaminin IgG. *Lab. Invest.* 52:169-181.
4. Abrahamson, D. R., and E. W. Perry. 1986. Evidence for splicing new basement membrane into old during glomerular development in newborn rat kidneys. *J. Cell Biol.* 103:2489-2498.
5. Abrahamson, D. R., A. Hein, and J. P. Caulfield. 1983. Laminin in glomerular basement membranes of aminonucleoside nephrotic rats: increased proteinuria induced by antilaminin immunoglobulin G. *Lab. Invest.* 49:38-47.
6. Andujar, M. B., H. Magloire, D. J. Hartmann, G. Ville, and J.-A. Grimaud. 1985. Early mouse molar root development: cellular changes and distribution. *Differentiation.* 30:111-122.
7. Aumailley, M., V. Nurcombe, D. Edgar, M. Paulsson, and R. Timpl. 1987. The cellular interaction of laminin fragments: cell adhesion correlates with two fragment-specific high affinity binding sites. *J. Biol. Chem.* 262:11532-11538.
8. Bender, B. L., R. Jaffe, B. Carlin, and A. E. Chung. 1981. Immunolocalization of entactin, a sulfated basement membrane component, in rodent tissues, and comparison with GP-2 (laminin). *Am. J. Pathol.* 103:419-426.
9. Courtoy, P. J., R. Timpl, and M. G. Farquhar. 1982. Comparative distribution of laminin, type IV collagen and fibronectin in the rat glomerulus. *J. Histochem. Cytochem.* 30:874-886.
10. Covault, J., J. M. Cunningham, and J. R. Sanes. 1987. Neurite outgrowth on cryostat sections of innervated and denervated skeletal muscle. *J. Cell Biol.* 105:2479-2488.
11. Dziadek, M., S. Fujiwara, M. Paulsson, and R. Timpl. 1985. Immunological characterization of basement membrane types of heparan sulfate proteoglycan. *EMBO (Eur. Mol. Biol. Organ) J.* 4:905-912.
12. Dziadek, M., M. Paulsson, and R. Timpl. 1985. Identification and interaction repertoire of large forms of the basement membrane protein nidogen. *EMBO (Eur. Mol. Biol. Organ.) J.* 4:2513-2518.
13. Edgar, D., R. Timpl, and H. Thoenen. 1984. The heparin-binding domain of laminin is responsible for its effects on neurite outgrowth and neuronal survival. *EMBO (Eur. Mol. Biol. Organ.) J.* 3:1463-1468.
14. End, P., G. Panayotou, R. Timpl, and J. Engel. 1987. Growth factor like domains in laminin. *Experientia (Basel).* 43:636.
15. Engel, J., and H. Furthmayr. 1987. Electron microscopy and other physical methods for the characterization of extracellular matrix components: laminin, fibronectin, collagen IV, collagen VI and proteoglycans. *Methods Enzymol.* 145:3-78.
16. Engel, J., E. Odermatt, A. Engel, J. A. Madri, H. Furthmayr, and R. Timpl. 1981. Shapes, domain organizations and flexibility of laminin and fibronectin, two multifunctional proteins of the extracellular matrix. *J. Mol. Biol.* 150:97-120.
17. Farquhar, M. A. 1981. The glomerular basement membrane: a selective macromolecular filter. *In* Cell Biology of Extracellular Matrix. E. D. Hay, editor. Plenum Press, New York. 335-378.
18. Fleischmajer, R., R. Timpl, M. Dziadek, and M. Lebwohl. 1985. Basement membrane proteins, interstitial collagens and fibronectin in neurofibroma. *J. Invest. Dermatol.* 85:54-59.
19. Foidart, J. M., E. W. Bere, M. Yaar, S. I. Rennard, M. Gullino, G. R. Martin, and S. I. Katz. 1980. Distributions and immunoelectron microscopic localisation of laminin, a noncollagenous basement membrane glycoprotein. *Lab. Invest.* 42:336-342.
20. Furthmayr, H., F. J., Roll, J. A. Madri, and H. Foellmer. 1982. Composition of basement membranes as viewed with the electron microscope. *In* New Trends in Basememt Membrane Research. K. Kühn, H. Schöne, and R. Timpl, editors. Raven Press, New York. 31-84.
21. Gil, J., and A. Martinez-Hernandez. 1984. The connective tissue of the rat

lung: electron immunohistochemical studies. *J. Histochem. Cytochem.* 32:230–238.

22. Goldberg, M., and F. Escaig-Haye. 1986. Is the lamina lucida of the basement membrane a fixation artefact? *Eur. J. Cell Biol.* 42:365–368.
23. Goodman, S. L., R. Deutzmann, and K. von der Mark. 1987. Two distinct cell-binding domains in laminin can independently promote nonneuronal cell adhesion and spreading. *J. Cell Biol.* 105:589–598.
24. Graf, J., Y. Iwamoto, M. Sasaki, G. R. Martin, and H. K. Kleinman. 1987. Identification of an amino acid sequence in laminin mediating cell attachment, chemotaxis and receptor binding. *Cell.* 48:989–996.
25. Griffiths, G., K. Simons, G. Warren, and K. T. Tokuyasu. 1982. Immunoelectron microscopy using thin frozen sections: applications to studies of the intracellular transport of Semliki forest virus spike glycoproteins. *Methods Enzymol.* 96:466–495.
26. Jakus, M. A. 1962. Further observations on the fine structure of the cornea. *Invest. Ophthalmol.* 1:202–225.
27. Kanwar, Y. S., and M. G. Farquhar. 1979. Anionic sites in the glomerular basement membrane. In vivo and in vitro localization to the laminae rarae by cationic probes. *J. Cell Biol.* 81:137–153.
28. Kleinman, H. K., F. B. Cannon, G. W. Laurie, J. R. Hassell, M Aumailley, V. P. Terranova, G. R. Martin, and M. Dubois-Dalcq. 1985. Biological activities of laminin. *J. Cell. Biochem.* 27:317–325.
29. Laurie, G. W., C. P. Leblond, S. Inoue, G. R. Martin, and A. Chung. 1984. Fine structure of the glomerular basement membrane and immunolocalisation of five basement membrane components to the lamina densa (basal lamina) and its extensions in both glomeruli and tubules of the rat kidney. *Am. J. Anat.* 169:463–481.
30. Laurie, G. W., C. P. Leblond, and G. R. Martin. 1982. Localization of type IV collagen, laminin, heparan sulfate proteoglycan, and fibronectin to the basal lamina of basement membranes. *J. Cell Biol.* 95:340–344.
31. Lesot, H., U. Kühl, and K. von der Mark. 1983. Isolation of a laminin-binding protein from muscle cell membranes. *EMBO (Eur. Mol. Biol. Organ.) J.* 2:861–865.
32. Madri, J. A., F. J. Roll, H. Furthmayr, and J.-M. Foidart. 1980. Ultrastructural localization of fibronectin and laminin in the basement membranes of the murine kidney. *J. Cell Biol.* 86:682–687.
33. Martin, G. R., and R. Timpl. 1987. Laminin and other basement membrane components. *Annu. Rev. Cell Biol.* 3:57–85.
34. Martinez-Hernandez, A. 1984. The hepatic extracellular matrix. I. Electron immunohistochemical studies in normal rat liver. *Lab. Invest.* 51:57–74.
35. Martinez-Hernandez, A. 1987. Electron immunohistochemistry for the extracellular matrix: an overview. *Methods Enzymol.* 145:78–103.
36. Martinez-Hernandez, A., and A. E. Chung, 1984. The ultrastructural localisation of two basement membrane components: entactin and laminin in rat tissues. *J. Histochem. Cytochem.* 32:289–298.
37. McLean, I. W., and P. K. Nakane. 1974. Periodate-Lysine-Paraformaldehyde fixative: a new fixative for immunoelectron microscopy. *J. Histochem. Cytochem.* 22:1077–1083.
38. Modesti, A., T. Kalebic, S. Scarpa, S. Togo, G. Grotendorst, L. A. Liotta, and T. J. Triche. 1984. Type V collagen in human amnion is a 12 nm fibrillar component of the pericellular interstitium. *Eur. J. Cell Biol.* 35:246–255.
39. Monaghan, P., M. J. Warburton, N. Perusinghe, and P. S. Rudland. 1983. Topographical arrangement of basement membrane proteins in lactating rat mammary gland: comparison of the distribution of type IV collagen, laminin, fibronectin and Thy-1 at the ultrastructural level. *Proc. Natl. Acad. Sci. USA.* 80:3344–3348.
40. Moor, H., G. Bellin, C. Slandri, and K. Akert. 1980. The influence of high pressure freezing on mammalian nerve tissue. *Cell Tissue Res.* 209:201–216.
41. Mynderse, L. A., J. R. Hassell, H. K. Kleinmann, G. R. Martin, and A. Martinez-Hernandez. 1983. Loss of heparan sulfate proteoglycan from glomerular basement membrane nephrotic rats. *Lab. Invest.* 48:292–302.
42. Deleted in proof.
43. Ott, U., E. Odermatt, J. Engel, H. Furthmayr, and R. Timpl. 1982. Protease resistance and conformation of laminin. *Eur. J. Biochem.* 123:63–72.
44. Paulsson, M. 1987. Noncollagenous proteins of basement membranes. *Collagen. Relat. Res.* 7:443–461.
45. Paulsson, M., M. Aumailley, R. Deutzmann, R. Timpl, K. Beck, and J. Engel. 1987. Laminin-nidogen complex: extraction with chelating agents and structural characterization. *Eur. J. Biochem.* 166:11–19.

46. Paulsson, M., R. Deutzmann, M. Dziadek, H. Nowack, R. Timpl, S. Weber, and J. Engel. 1986. Purification and properties of intact and degraded nidogen obtained from a tumor basement membrane protein. *Eur. J. Biochem.* 137:455–465.
47. Paulsson, M., M. Dziadek, C. Suchanek, W. Huttner, and R. Timpl. 1985. Nature of sulfated macromolecules in mouse Reicherts membrane. Evidence for tyrosine-O-sulfate in basement membrane proteins. *Biochem. J.* 231:571–579.
48. Paulsson, M., S. Fujiwara, M. Dziadek, R. Timpl, G. Pejler, G. Backström, U. Lindahl, and J. Engel. 1985. Structure and function of basement proteoglycans. *Ciba Found. Symp.* 124:189–203.
49. Paulsson, M., P. D. Yurchenco, G. C. Ruben, J. Engel, and R. Timpl. 1987. Structure of low density heparan sulfate proteoglycan isolated from a mouse tumor basement membrane. *J. Mol. Biol.* 197:297–313.
50. Pratt, B. M., and J. A. Madri. 1985. Immunolocalization of type IV collagen and laminin in nonbasement membrane structures of murine corneal stroma. *Lab. Invest.* 52:650–656.
51. Rao, C. N., I. M. K. Margulies, and L. A. Liotta. 1985. Binding domain for laminin on type IV collagen. *Biochem. Biophys. Res. Commun.* 128:45–52.
52. Roth, J. 1984. Light and electron microscopic localization of antigenic sites in tissue sections by the protein A-gold technique. *Acta Histochem.* 29 (Suppl):9–22.
53. Sandrock, A. W., Jr., and W. D. Matthew. 1987. An in vitro neurite-promoting antigen functions in axonal regeneration in vivo. *Science (Wash. DC).* 237:1605–1607.
54. Sanes, J. R. 1982. Laminin, fibronectin, and collagen in synaptic and extrasynaptic portions of muscle fiber basement membrane. *J. Cell Biol.* 93:442–451.
55. Sasaki, M., and Y. Yamada. 1987. The laminin B2 chain has a multidomain structure homologous to the B1 chain. *J. Biol. Chem.* 262:17111–17117.
56. Sasaki, M., S. Kato, K. Kohno, G. R. Martin, and Y. Yamada. 1987. Sequence of cDNA encoding the laminin B1 chain reveals a multidomain protein containing cysteine-rich repeats. *Proc. Natl. Acad. Sci. USA.* 84:935–939.
57. Schiff, R., and J. Rosenbluth. 1986. Ultrastructural localization of laminin in rat sensory ganglia. *J. Histochem. Cytochem.* 34:1691–1699.
58. Schittny, J. C. 1987. Aspekte der strukturellen Organisation der Basalmembran und der Mauscornea. Doctoral Thesis, University of Basel, Basel, Switzerland. 57–59.
59. Semoff, S., B. L. M. Hogan, and C. R. Hopkins. 1982. Localisation of fibronectin, laminin-entactin, and entactin in Reichert's membrane by immunoelectron microscopy. *EMBO (Eur. Mol. Biol. Organ.) J.* 1:1171–1175.
60. Stephens, H., M. Bendayan and V. Gisiger. 1985. Simultaneous labeling of basal lamina components and acetylcholinesterase at neuromuscular junction. *Histochem. J.* 17:1203–1220.
61. Stephens, H., M. Bendayan, and M. Silver. 1982. Immunocytochemical localisation of collagen types and laminin in skeletal muscle with the protein A-gold technique. *Biol. Cell.* 44:81–84.
62. Terranova, V. P., C. N. Rao, T. Kalebic, M. L. Margulies, and L. A. Liotta. 1983. Laminin receptor on human breast carcinoma cells. *Proc. Natl. Acad. Sci. USA.* 80:444–448.
63. Timpl, R. 1982. Antibodies to collagens and procollagens. *Methods Enzymol.* 82:472–498.
64. Timpl, R., and M. Dziadek. 1986. Structure, development, and molecular pathology of basement membranes. *Int. Rev. Exp. Pathol.* 1–112.
65. Timpl, R., M. Dziadek, S. Fujiwara, H. Nowack, and G. Wick. 1983. Nidogen: a new self-aggregating basement membrane protein. *Eur. J. Biochem.* 137:455–465.
66. Timpl, R., M. Paulsson, M. Dziadek, and S. Fujiwara. 1987. Basement membranes. *Methods Enzymol.* 145:363–391.
67. Timpl, R., H. Wiedemann, V. Van Delden, H. Furthmayr, and K. Kühn. 1981. A network model for the organization of type IV collagen molecules in basement membranes. *Eur. J. Biochem.* 120:203–211.
68. Tohyama, K., and C. Ide. 1984. The localization of laminin and fibronectin on the Schwann cell basal lamina. *Arch. Histol. JPN.* 47:519–532.
69. Yurchenco, P. D., and G. C. Ruben. 1987. Basement membrane structure in situ: evidence for lateral associations in the type IV collagen network. *J. Cell Biol.* 105:2559–2568.
70. Yurchenco, P. D., E. C. Tsilibary, A. S. Charonis, and H. Furthmayr. 1986. Models for the self-assembly of basement membrane. *J. Histochem. Cytochem.* 34:93–102.